Czech Technical University in Prague
Faculty of Mechanical Engineering

Summary of Ph.D. Thesis

NUMERICAL SOLUTION OF FLOW IN TURBINE CASCADES AND STAGES

Ing. Jan Halama

Supervisor:
Doc.Ing. Jaroslav Fořt, CSc.

Branch of science:
Mathematical and Physical Engineering

2003

The Ph.D. thesis is the outcome of a full-time internal doctoral study program at the Department of Technical Mathematics, Faculty of Mechanical Engineering, Czech Technical University in Prague.

Disertant: Ing. Jan Halama

Supervisor: Doc. Ing. Jaroslav Fořt, CSc.

Opponents:

The thesis was sent out on:

The defense of the dissertation will take place on:

in room No. 17, Faculty of Mechanical Engineering, Technická 4, Praha 6 - Dejvice, in front of the appointed ad hoc committee in the study program Mathematical and Physical Engineering. The thesis is available in the Department of Science and Research of Mechanical Engineering Faculty, Czech Technical University in Prague, Technická 4, Praha 6 - Dejvice.

Prof. RNDr. Karel Kozel, DrSc.
Head of Doctoral Study Program
Mathematical and Physical Engineering
Czech Technical University in Prague
Faculty of Mechanical Engineering

Anotace

Tato práce se zabývá numerickým řešením transsonického proudění v turbínových mřížích a stupních. Vlastnosti použitých numerických schémat jsou analyzovány pomocí modifikovaných rovnic pro skalární případy, včetně rovnice se zdrojovým členem a nestacionární metody 'fractional step'. Numerická realizace výpočtu na neperiodické více-blokové síti je prezentována. Vhodná matematická formulace a numerická aproximace okrajových podmínek je diskutována pro případy proudění v turbínových mřížích a stupních. Případ výstupní okrajové podmínky je popsán podrobněji. Vliv použité sítě, diskretizace a okrajových podmínek je zmíněn. Formulace a numerické řešení 3D nestacionární interakce statoru s rotorem na pohybujících se sítích jsou navrženy a testovány pro vhodné případy reálného proudění. Rovnice popisující vícefázové proudění mají z matematického hlediska 'stiff' charakter kvůli rychlým fázovým změnám. Proto je navržena speciální varianta 'fractional step' metody s různými časovými kroky pro jednotlivé podproblémy. Tato numerická metoda je analyzována pro případ 1D nestacionárních operátorů. Použitelnost prezentovaných numerických metod pro případy reálného proudění je ověřena pomocí porovnání numerických výsledků s dostupnými experimentálními daty stejně jako s numerickými výsledky jiných autorů. Prezentovaná práce zahrnuje výsledky numerického řešení různých reálných případů proudění (spolupráce s PBS Velká Bíteš, Škoda Plzeň a Von Kármánovým institutem). Dosažené numerické výsledky jsou v dobré shodě s výsledky jiných autorů a s experimentálními daty.

Abstract

This work deals with a numerical solution of a transonic flow in turbine cascades and stages. The properties of used numerical schemes are analyzed by means of modified equations for scalar cases including also the cases of the equation with a source term and an unsteady fractional step method. A numerical realization of computation on a non-periodic multi-block grid is presented. Appropriate mathematical formulation and numerical approximation of boundary conditions are discussed for the cases of flow in turbine cascades and stages. The case of outlet boundary condition is described in more details. The influence of used grid, discretization and boundary conditions is mentioned. The formulation and the numerical solution of a 3D unsteady stator/rotor interaction problem on moving grids are proposed and tested on appropriate real flow cases. The equations describing the multiphase flow have from mathematical point of view stiff character due to the fast phase changes. Therefore a particular version of a fractional step method with the different time steps for individual sub-problems is proposed. This numerical method is analyzed for 1D unsteady operators. The applicability of all presented numerical methods for real flow cases is verified by a comparison of numerical results with available experimental data as well as with numerical results of other authors. Presented work includes results of numerical solution of different real flow problems (cooperation vith PBS Velká Bíteš, Škoda Pilsen and Von Kármán Institute). Obtained numerical results are in a good agreement with the results of other authors and with experimental data.

List of symbols

Alphanumeric symbols:

a	$[m\ s^{-1}]$	speed of sound
c_p	$[J\ kg^{-1}K^{-1}]$	specific heat at constant pressure
e	$[J\ m^3]$	total energy per unit volume
J	$[m^{-3}s^{-1}]$	nucleation rate
$\mathcal{J}$	$[-]$	complex unit
Kn	$[-]$	Knudsen number
L	$[J\ kg^{-1}]$	latent heat
M	$[-]$	Mach number
p	$[Pa]$	pressure
q	$[W\ m^{-2}]$	heat flux
r	$[m]$	r–coordinate, droplet radius
R	$[J\ kg^{-1}K^{-1}]$	gas constant
t	$[s]$	time
T	$[K]$	temperature
T	$[s]$	time period
$\hat{T}$	$[^\circ C]$	temperature
u	$[m\ s^{-1}]$	velocity
w	$[-]$	wetness
x	$[m]$	x–coordinate
y	$[m]$	y–coordinate
z	$[m]$	z–coordinate

Greek symbols:

η	$[Pa\ s]$	dynamic viscosity
φ	$[-]$	φ–coordinate
γ	$[-]$	ratio of specific heats
λ	$[W\ K^{-1}m^{-1}]$	thermal conductivity
Ω	$[s^{-1}]$	angular velocity
ρ	$[kg\ s^{-1}]$	density
σ	$[N\ m^{-1}]$	surface tension
τ	$[Pa]$	shear stress

Superscripts:

$\cdot^n$	discrete time
$\cdot'$	physical quantity

Subscripts:

- $\cdot_0$ total
- $\cdot_\varphi$ φ–component
- $\cdot_c$ critical
- $\cdot_i$ grid index
- $\cdot_{is}$ isentropic
- $\cdot_j$ grid index
- $\cdot_l$ liquid
- $\cdot_r$ r–component
- $\cdot_R$ rotor
- $\cdot_s$ saturation
- $\cdot_S$ stator
- $\cdot_t$ time derivative
- $\cdot_v$ vapor
- $\cdot_x$ x–component, x–derivative
- $\cdot_y$ y–component, y–derivative
- $\cdot_z$ z–component, z–derivative

Contents

1 Introduction, present state of numerical modelling of flow in turbines

This work deals with a numerical solution of transonic flow in turbine cascades and stages. Up to now there are still no available theoretical results for the existence and the uniqueness of physically acceptable solution of compressible flow problems. An analysis of numerical methods is limited only to the case of a scalar equation for one or eventually more space variables. Obtained theoretical results are then extended to multi-D problems.

Since a numerical modelling of flow takes nowadays a place during the whole design procedure of any turbine, we have to solve numerically 2D, quasi-3D or 3D either steady or unsteady Euler or Reynolds averaged Navier-Stokes equations, which can be further completed by additional equations describing the effects of turbulence, condensation, chemical reaction etc. Moreover the real structure of turbomachinery flows is generally very complex, it includes such phenomena as limited flow rate, shock waves, shear layers, condensation, secondary flow effects etc. This means we have first to choose such flow model, which is an appropriate approximation of the real flow and which can be solved numerically, it mean e.g. which allows the use of physically acceptable and numerically realizable boundary conditions. Results obtained by any numerical method can be then of course analyzed only within the limits of this flow model.

A numerical method has to be chosen according to the properties of equations of a used flow model. Before one can rely on results of numerical method he has at least to verify the influence of grid (grid type, number of grid points, cell aspect ratio, grid refinement, cell deformation, ...), the influence of used discretization (there are different ways how to discretize convection, dissipation and production terms) and the influence of boundary (a proper type of boundary conditions, position of boundary, ...). This verification is possible either by using several independent numerical methods or/and precise experimental data. Praxis shows that there is no universal numerical method.

Some of currently investigated problems are: a proper higher order discretization of convective term; inflow and outflow boundary conditions; turbulence modelling; interaction of blade cascades, coupling of Euler and Navier-Stokes equations with other equations describing condensation, blade vibrations, chemical reactions, combustion, etc.

The different types of inflow and outflow boundary conditions are limited to certain cases. Giles [32] published non-reflecting boundary conditions for the inflow and the outflow boundary for explicit cell-vertex schemes and for 2D axial cascades. These conditions were extended to 3D by Saxer [55]. Magagnato recently tested the use of buffer layer technique for internal aerodynamics, however he reported big problems in [50].

It is known that for the flow in turbine stages steady flow models yield results different from the time-averages of results of unsteady flow models. This fact motivates the development of methods modelling the cascade interactions, e.g. Laumert et al [47], Jung et al [42].

The Euler or Navier-Stokes equations for a two-phase flow are coupled with the conservation equations for droplets for the modeling of two-phase flow of vapor with condensed

droplets. Some authors model the droplet spectra by dividing droplets into several classes according to droplet radius, e.g. Young [66]. However for multi-D problems with complex geometry it is mainly considered the average radius (only one droplet class), e.g. Šejna [60], Schnerr [56] or Dykas [16].

Praxis (author's stays, participation at international conferences on flow modelling and private discussions) shows that the successful use of complex flow solvers (either commercial or in-house) is conditioned by the user experiences and 'feeling', since they contain many parameters, which has to be tuned using several test cases. The big advantage of in-house codes against the commercial ones is, that the the existence of these parameters is known and they can be easily modified directly in the source code. Moreover some parameters in commercial codes are adjusted to provide a stable solution in any case, regardless if it is physically acceptable. These facts promotes the development of own in-house numerical codes, although they necessarily start from simple problems and their development takes several years.

The numerical methods applied for the calculation of flow in turbine cascades and stages in this work are mainly based on the Lax-Wendroff type schemes, therefore in the first part we analyze their properties (numerical stability and the dispersive/dissipative behaviour) for a different linear scalar partial differential equations modelling the pure convection, the convection-diffusion and the convection-production flow problems. Further it follows a description of an extension of finite difference methods from linear to non-linear cases. Conclusions drawn for finite difference methods for linear scalar equations presented in the first part are used for the analysis of properties of finite volume methods for multidimensional nonlinear problems (the choice of discretization, the estimates for the time step, the choice of splitting, ...).

The second part deals with the numerical solution of an inviscid and a laminar transonic flow in turbine cascades modelled by the Euler or the Navier-Stokes equations respectively. The used finite volume method for structured grids is based on the Lax-Wendroff scheme described in the first part. an appropriate mathematical formulation and a numerical approximation of boundary conditions are discussed for the cases of flow in 2D/3D axial/radial turbine cascades. The mathematical formulation and the numerical realization of outlet boundary condition for the case of flow with shock waves in the outlet part is described in more details. Further a numerical realization of computation on a non-periodic multi-block grid is presented. A particular attention is paid to the quality of computational grid. The applicability of used numerical method for real flow cases has been verified by means of numerical results of an inviscid and a laminar 2D flow in the axial stator cascade SE 1050 (QNET network); an inviscid 2D flow in radial stator and rotor cascades computed in the frame of cooperation with the PBS Velká Bíteš; an inviscid 3D flow in axial stator and rotor of the last stage of 1000 MW turbine Škoda computed in the frame of cooperation with the Škoda Pilsen; and a laminar 3D flow in a curved channel.

The formulation and the numerical solution of 3D unsteady stator/rotor interaction problem on moving grids are proposed in the third part. Other numerical techniques, which can be used for the modelling of the unsteady stator/rotor interaction, are also mentioned. The finite volume method, which was developed during the author's stay at

Von Kármán Institute is described. This method was validated by the comparison of numerical results with the experimental data for the NASA and BRITE (BRITE-EURAM program) stages.

The fourth part deals with a transonic flow of wet steam. It starts with the description of a model of condensation, which is based on the Šejna's model [60]. However several material properties which were in the Šejna's model considered as constants are taken as functions of temperature (e.g. specific heat ratio). Improvements of the relation for nucleation rate as well as modifications improving the original Hill's approximation [38] for the description of droplets are presented. The equations describing the wet steam flow have from mathematical point of view stiff character due to the fast phase changes. Therefore a particular version of fractional step method with the different time steps for individual sub-problems is proposed. This method is analyzed in the firts part using the scalar equation as well as by 1D operators. Numerical results of quasi-2D and 2D transonic flow of condensing steam in convergent-divergent nozzle are compared with the experimental data of Barschdorff [8] as well as with the numerical data of Dykas [16]. Finally, numerical results of 2D inviscid and laminar transonic flow of condensing steam in the axial turbine cascade SE 1050 are discussed.

2 The goals

The goals of the presented work are:

1. to analyze properties of the Lax-Wendroff scheme for the linear scalar equations modelling the pure convection, the convection-diffusion and the convection-production flow problems by means of the finite difference method, eventually to find possible improvements of this scheme for particular flow problems.

2. to develop and to validate a finite volume method for the solution of an inviscid and a viscous flow, i.e. to find an appropriate mathematical formulation and numerical realization of boundary conditions for a transonic flow in 2D/3D axial/radial stator/rotor cascades, to find a proper artificial dissipation term with regards to applicability to real flow cases ($Re \approx 10^6$), and to find a suitable type of a computational grid.

3. to propose an appropriate problem formulation for the case of unsteady stator-rotor interaction on moving grids, and to develop and to validate a finite volume method for the solution of 3D unsteady inviscid stator-rotor interaction in axial stage.

4. to propose a suitable problem formulation for the case of two-phase flow of condensing steam in complex geometries, to develop and to analyze a numerical method for the solution of stiff problem of two-phase flow of condensing steam, and to validate the numerical method using suitable real flow cases (inviscid and laminar 2D flow of condensing steam in nozzles and turbine cascades).

3 Scalar equations for model problems

Finite volume methods applied for multi-D flow problems are based on finite difference methods for corresponding scalar equations. We draw an attention in the following scalar equations: a pure convection equation (it corresponds to an inviscid flow without body forces), a convection-diffusion equation (it models a viscous flow without body forces) and a convection-production equation (it represents an inviscid flow with a source term due to body forces or with a condensation). For each case we analyze first the Lax-Wendroff scheme for a linear problem. Stability conditions are derived using the Von Neumann spectral analysis and a truncation errors are checked by means of modified equations, which also provide an information about dispersive or dissipative behavior of schemes. Moreover two different artifical dissipation terms are discussed (stability conditions, modified equations) and a further numerical scheme (Runge-Kutta scheme) is shown. Possible extensions of schemes for a nonlinear problems are also presented. For a convection-diffusion equation is discussed the discretization of diffusion term. In the part describing a convection-production equation it is presented not only a Lax-Wendroff scheme, but also a fractional step method based on the Lax-Wendroff scheme for the pure convection part and the Runge-Kutta scheme for the production part. Both numerical methods are compared from the point of view of stability and of truncation error. Furthermore a two different splitting techniques in the fractional step method are discussed.

4 Transonic flow in cascades

The inviscid flow model (the Euler equations) helps to validate the discretization of convective terms. It also yields a basic idea about the influence of computational grid and about the adjustment of artificial viscosity coefficients. Moreover it provides a valuable information about the flow with a dominant potential effect (accelerated flow without separation). The laminar flow model (the Navier-Stokes equations) for a high Reynolds number flow is an artificial step in the development of a method for a turbulent flow. It helps to verify the grid influence, the discretization of viscous terms and the applicability of numerical method for high Reynolds number flows (balance between physical and artificial viscosity).

A numerical method is based on a cell-vertex finite volume discretization and the Lax-Wendroff scheme.

4.1 Governing equations, numerical method

A laminar transonic flow is modelled by the system of Navier-Stokes equations (1) – equations are written in the Cartesian frame which can rotate around x–axis at a constant angular velocity Ω. The system of equations is closed by the relation (3) for the pressure p.

$$\frac{\partial}{\partial t}\mathbf{W} = -\frac{\partial}{\partial x}\mathbf{F}^c + \frac{\partial}{\partial x}\mathbf{F}^v - \frac{\partial}{\partial y}\mathbf{G}^c + \frac{\partial}{\partial y}\mathbf{G}^v - \frac{\partial}{\partial y}\mathbf{H}^c + \frac{\partial}{\partial y}\mathbf{H}^v + \mathbf{P}, \tag{1}$$

$$
\begin{aligned}
\mathbf{W} &= [\rho, \rho u_x, \rho u_y, \rho u_z, e]^T, \\
\mathbf{F}^c &= [\rho u_x, \rho u_x^2 + p, \rho u_x u_y, \rho u_x u_z, (e+p)u_x]^T, \\
\mathbf{F}^v &= [0, \tau_{xx}, \tau_{xy}, \tau_{xz}, u_x\tau_{xx} + u_y\tau_{xy} + u_z\tau_{xz} - q_x]^T, \\
\mathbf{G}^c &= \left[\rho u_y, \rho u_y u_x, \rho u_y^2 + p, \rho u_y u_z, (e+p)u_y\right]^T, \\
\mathbf{G}^v &= [0, \tau_{xy}, \tau_{yy}, \tau_{yz}, u_x\tau_{xy} + u_y\tau_{yy} + u_z\tau_{yz} - q_y]^T, \\
\mathbf{H}^c &= [\rho u_z, \rho u_z u_x, \rho u_z u_y, \rho u_z^2 + p, (e+p)u_z]^T, \\
\mathbf{H}^v &= [0, \tau_{xz}, \tau_{yz}, \tau_{zz}, u_x\tau_{xz} + u_y\tau_{yz} + u_z\tau_{zz} - q_z]^T, \\
\mathbf{P} &= [0, 0, \rho(\Omega^2 y - 2\Omega u_z), \rho(\Omega^2 z + 2\Omega u_y), 0]^T,
\end{aligned}
\tag{2}
$$

$$
p = (\gamma - 1)\left[e - \frac{1}{2}\rho\left(u_x^2 + u_y^2 + u_z^2\right) + \frac{1}{2}\rho\Omega^2(y^2 + z^2)\right], \tag{3}
$$

where the symbol ρ denotes density, u_x, u_y and u_z velocity components, p pressure, e total energy per unit volume, τ shear stress, q heat flux, t time, x, y and z the spatial coordinates, γ the specific heat ratio, superscripts $\cdot^c$ the convective and $\cdot^v$ the viscous fluxes.

The domain of solution $D \subset R^3$ for a cascade flow calculations consist usually of one blade passage. The solution $\mathbf{W} : D \to R^5$ has to fulfill the integral form (4) of equation (1) for any subset $V \subset D$ and boundary conditions along boundary ∂D.

$$
\frac{\partial}{\partial t}\iiint_{V_{i,j,k}} \mathbf{W}\, dV = -\iiint_{V_{i,j,k}} (\mathbf{F}_x + \mathbf{G}_y + \mathbf{H}_z - \mathbf{P})\, dV. \tag{4}
$$

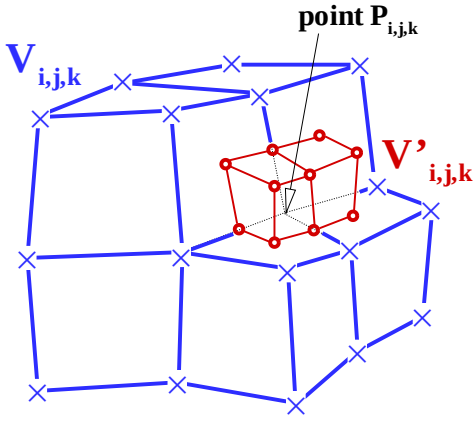

Figure 1: Finite volumes $V_{i,j,k}$ and $V'_{i,j,k}$

The cell-vertex finite volume method based on the Lax-Wendroff scheme on structured

hexahedral grid can be written in the following two steps

$$\mathbf{W}_t\big|_{i,j,k}^n = -\frac{1}{\mu(V_{i,j,k})}\oiint_{\partial V_{i,j,k}} (\mathbf{F}^{(1)}, \mathbf{G}^{(1)}, \mathbf{H}^{(1)})\ \vec{n}_{\partial V} dS + \frac{1}{\mu(V_{i,j,k})}\iiint_{V_{i,j,k}} \mathbf{P} dV$$

$$\mathbf{W}_{i,j,k}^{n+1} = \mathbf{W}_{i,j,k}^n + \Delta t \mathbf{W}_t\big|_{i,j,k}^n + \frac{\Delta t^2}{2\mu(V'_{i,j,k})}\iiint_{V'_{i,j,k}} \mathbf{P}_{\mathbf{W}} \mathbf{W}_t\big|_{i,j,k}^n\ dV' - \tag{5}$$

$$-\frac{\Delta t^2}{2\mu(V'_{i,j,k})}\oiint_{\partial V'_{i,j,k}} \left(\mathbf{F}_{\mathbf{W}}^{(0)}\mathbf{W}_t\big|_{i,j,k}^n, \mathbf{G}_{\mathbf{W}}^{(0)}\mathbf{W}_t\big|_{i,j,k}^n, \mathbf{H}_{\mathbf{W}}^{(0)}\mathbf{W}_t\big|_{i,j,k}^n\right)\vec{n}_{\partial V} dS' + \mathcal{DIS}_{i,j,k}^n,$$

where

$$\mathbf{F}^{(\xi)} = \mathbf{F}^c - \xi\mathbf{F}^v, \qquad \mathbf{G}^{(\xi)} = \mathbf{G}^c - \xi\mathbf{G}^v, \qquad \mathbf{H}^{(\xi)} = \mathbf{H}^c - \xi\mathbf{H}^v \tag{6}$$

and the symbols $\mathbf{F}_{\mathbf{W}}$, $\mathbf{G}_{\mathbf{W}}$, $\mathbf{H}_{\mathbf{W}}$ and $\mathbf{P}_{\mathbf{W}}$ denote Jacobi matrices. According to the scheme for scalar equation the Jacobi matrixes are evaluated only for inviscid fluxes ($\xi = 0$). The $\mathcal{DIS}_{i,j,k}^n$ is the conservative form of artificial viscosity term with the second and fourth order derivatives according to Stringer and Morton [59]

For the evaluation of shear stresses τ and of heat fluxes q we need all space derivatives of all velocity components and of temperature T. The x-derivatives are calculated as follows

$$\frac{\partial}{\partial x}\begin{bmatrix} u_x \\ u_y \\ u_z \\ T \end{bmatrix}\Bigg|_{i,j,k} = \frac{1}{\mu(V_{i,j,k})}\iiint_{V_{i,j,k}} \frac{\partial}{\partial x}\begin{bmatrix} u_x \\ u_y \\ u_z \\ T \end{bmatrix} dV = \frac{1}{\mu(V_{i,j,k})}\oiint_{\partial V_{i,j,k}} \begin{bmatrix} u_x \\ u_y \\ u_z \\ T \end{bmatrix} n_{\partial V}^x\ dS, \tag{7}$$

the y and z-derivatives are calculated analogically. For practical use all integrals are replaced by sums over cell volume or faces. We have also tested a numerical method, where the time derivatives of fluxes are not calculated using Jacobi matrixes, but numerically.

We use structured quadrilateral (2D) or hexahedral (3D) grids. The simplest structured grid is the algebraically generated H-type grid, which can be generated very easily, however it discretizes poorly the leading and trailing edge regions, especially for thick leading and trailing edges. Improvements of the discretization of leading and trailing edge regions can be reached by using the H-type mesh created by elliptic generator. Further improvements brings the O-H multi-block grid, which eliminates the grid distortion close to leading and trailing edges.

The component of inlet velocity, which is normal to the inlet boundary, is considered to be subsonic. Therefore according to the theory of characteristics we have to prescribe '*number of unknowns minus one*' parameters and to take '*one*' from a solution domain at the inlet boundary. The implementations for particular cases of flow in 2D/3D stator/rotor cascades are described.

The component of outlet velocity, which is normal to outlet boundary, is also considered to be subsonic, therefore according to the theory of characteristic we have to prescribe

'*one*' parameter and to take '*number of unknowns minus one*' from a solution domain. The simplest implementations of this condition is a constant value of pressure p_{out} along the whole outlet boundary. Since this condition ignores any pressure gradient along the outlet boundary, its use for transonic flow (unphysical shock reflections) and for radial cascades (outlet boundary is very close to trailing edges) is very limited. The aim of the so called non-reflecting boundary condition is to suppress the influence of the flow field by the position of computational domain boundary. One of the possibilities for cell-vertex methods is the formulation published by Giles [32] and [34]. The non-reflecting outlet boundary condition of Giles is relatively complicated and it was derived for axial cascade, cell-vertex finite volumes and uniformly spaced grid points along the outlet boundary. We propose simpler condition (further called 'integral of pressure'), which can be used for any type of finite volumes and it is not limited to axial case as well as to uniform spacing of grid points, see 2D Eq.(8), where $0 < \zeta \leq 1$ is relaxation parameter.

$$\begin{aligned} p_j &= f(\mathbf{W}^{n+1}_{imax,j}) \\ p^*_j &= (1-\zeta)\cdot p_j + \zeta \cdot p_j \cdot \frac{p_{out}}{\overline{p_j}} \\ e^{n+1,\ corrected}_{imax,j} &= f(\rho^{n+1}_{imax,j}, \vec{u}\,^{n+1}_{imax,j}, p^*_j) \end{aligned} \tag{8}$$

This condition yields the same flow field structure like the non-reflecting outlet boundary condition of Giles.

4.2 Inviscid flow in 2D axial cascade

Numerical results of inviscid flow in 2D axial cascade show the grid influence. The algebraically generated H-type grid causes an unphysical production of entropy at the leading and the trailing edges, which can be seen as a distortion of isolines of the Mach number close to the profile and a wake-like structure downstream the trailing edge. An elliptic H-type grid suppresses the unphysical entropy production at the leading edge, however the wake-like layer, is still strong. The O-H multi-block grid suppresses also the wake-like layer. Presented results show, that for the discretization of leading edge is important a sufficient number of grid points, while the grid distortion is not of a great importance. The discretization of trailing edge region is also discussed.

4.3 Inviscid flow in 2D radial cascades

Flow parameters like flow angle, static pressure, etc. in the case of spiral flow (flow in radial cascades) depend on radius, i.e. unlike to axial cascades we cannot prescribe the same boundary conditions if we shift the inlet or the outlet boundary. Moreover the outlet boundary radius cannot be smaller than critical radius (radius, at which the radial velocity becomes sonic). Since the parameters necessary for the boundary conditions are not usually available at required radius they must be recalculated, see Fořt [18].

There is a lack of experimental data available for the radial cascades. The design of these cascades is mainly based on the knowledge of axial cascades. Numerical results

therefore yield valuable information. We present a sample of numerical results computed within the frame of the cooperation with PBS Velká Bíteš. The numerical results show the inviscid transonic flow in two plane cascades, one axial and one radial (see Fig. 2), with the same throat to chord ratio and composed of the same blade profiles. The equivalent boundary conditions were imposed for both cascades. The calculations of flow in radial cascade takes into account Coriolis and centrifugal forces. The effect of blade channel convergence as well as the effect of rotation are discussed. Numerical results show that the radial configuration provides a higher work output.

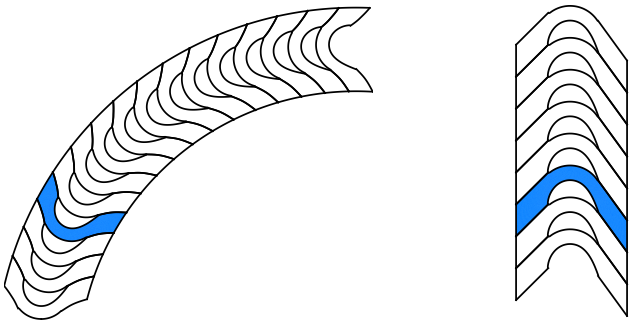

Figure 2: Radial (left) and axial (right) configuration.

4.4 Inviscid flow in 3D axial cascades

The numerical results of transonic flow in 3D axial turbine stator from the low pressure steam turbine stage of Škoda Pilsen Turbines show the abilities of presented cell-vertex numerical method to cope with a complex 3D geometry (big divergence of tip casing). Used algebraic H-type grid has about $5 \cdot 10^4$ points. Constant values of stagnation quantities and axial flow direction have been imposed at the stator inlet. Outlet static pressure has been prescribed as a function of radius. The figure 3 show the blade geometry and isolines of Mach number in three cuts for TVD MacCormack scheme (Fürst [27], constant outlet pressure), former cell-vertex scheme (artificial dissipation term according to Fořt et al [25], constant outlet pressure) and presented cell-vertex scheme (integral of pressure in the pitch-wise direction at the outlet). We can observe a relatively good agreement in flow field structure for all schemes. The constant pitch-wise distribution of the outlet pressure for the TVD MacCormack and for the former cell-vertex method causes a visible distortions of Mach number isolines. Presented results show that the presented cell-vertex method is less dissipative than the former one and that the integral of pressure at the outlet is applicable also for 3D steady case.

The flow in a rotor cascade with highly twisted blades from the same stage as the previous stator has been computed in relative frame of reference. Radial distributions of total relative density $\rho_{rel,0}$, total relative speed of sound $a_{rel,0}$ and relative flow angles, which we prescribe at the rotor inlet, were computed from $\mathbf{W}$ at the stator outlet and from angular velocity Ω.

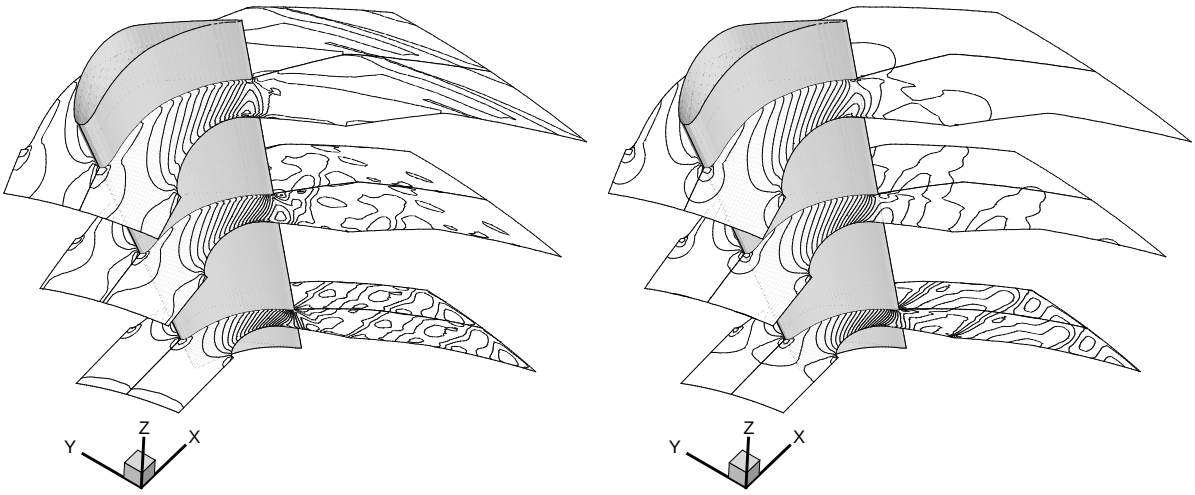

(a) TVD MacCormack scheme, Fürst [27] (b) the former cell-vertex method

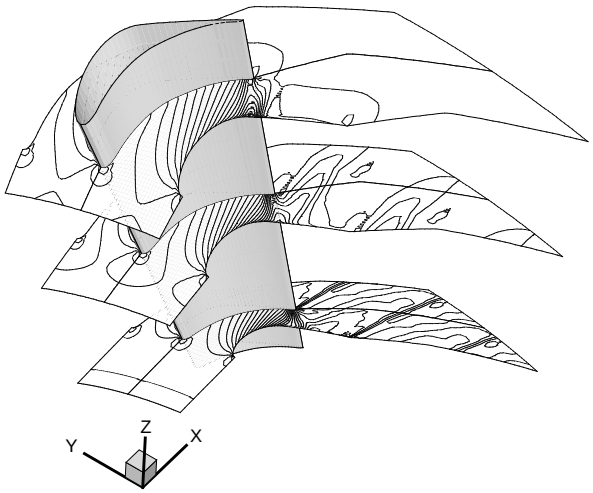

(c) the presented cell-vertex method

Figure 3: 3D turbine stator, isolines of Mach number ($\Delta M = 0.05$) in three grid planes 15%, 50% and 85% of span from the hub.

The figure 4 shows the isolines of relative Mach number obtained by TVD MacCormack scheme (Fürst [27], the frozen rotor case) and the former cell-vertex method for both the frozen rotor case (Coriolis and centrifugal forces are not taken into account) and the rotating rotor case. We can see a relatively good agreement in flow field structure for the frozen rotor case for the both methods. The results computed by the former cell-vertex method show the influence of rotation (compare the frozen and the rotating rotor cases). This influence is most dominant at the rotor hub.

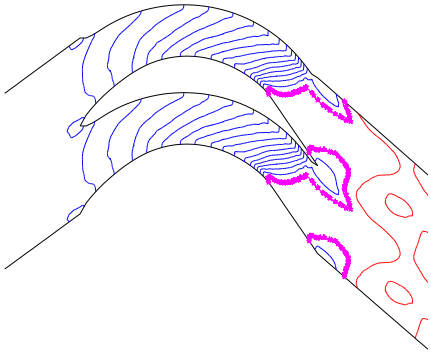

(a) TVD MacCormack scheme, Fürst [27], the frozen rotor case.

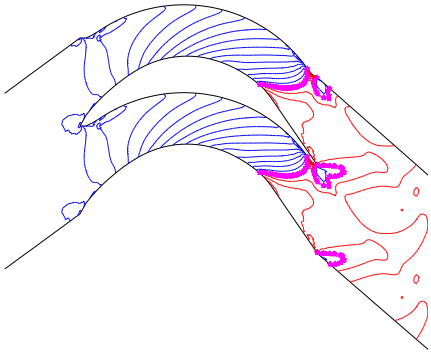

(b) the former cell-vertex method, the frozen rotor case.

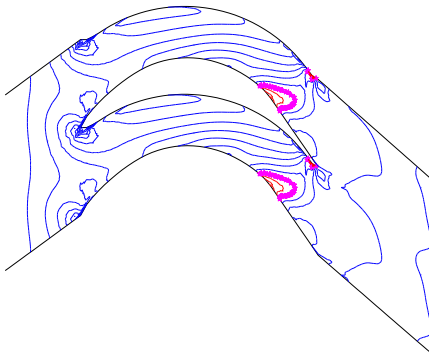

(c) the former cell-vertex method, the rotating rotor case.

Figure 4: 3D turbine rotor, isolines of relative Mach number ($\Delta M = 0.05$, marked isoline denotes the sonic line) in the grid plane located at the hub.

4.5 Laminar flow in 2D axial cascade SE1050

Although the laminar flow model is artificial for high Reynolds numbers, its numerical solution shows the applicability of methods for high Reynolds number flow calculations. After this necessary step, the presented method will be in future extended for a computation of turbulent flows.

The comparison of numerical results obtained by the presented cell-vertex method with the results of Roe scheme (Dobeš et al [12]) for $Re = 1.5 \cdot 10^6$ is shown in the Fig. 5. The same elliptical H-type grid was used for the both methods. The overall agreement of numerical results is good. The pressure distribution along the blade profile obtained by the presented cell-vertex method fits better the experimental data. The comparison with the experimental data is possible also for the results of laminar flow model, because Šťastný and Šafařík reported in [62] that the boundary layer is laminar along the whole pressure side and on the suction side it is laminar up to re-compression domain.

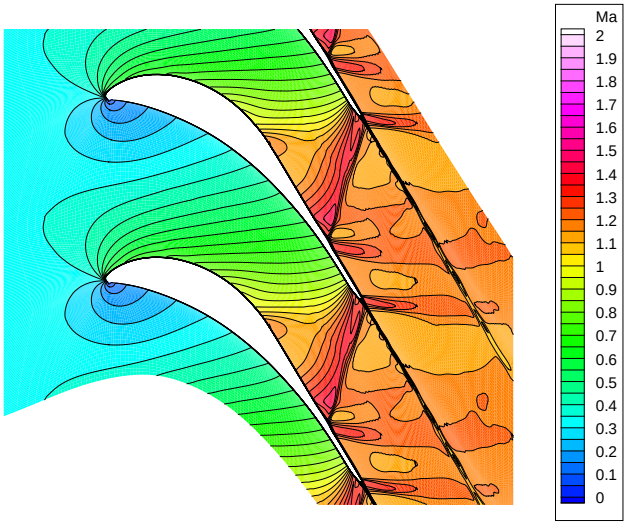

(a) laminar flow model, Mach number isolines, Roe scheme (Dobeš [12])

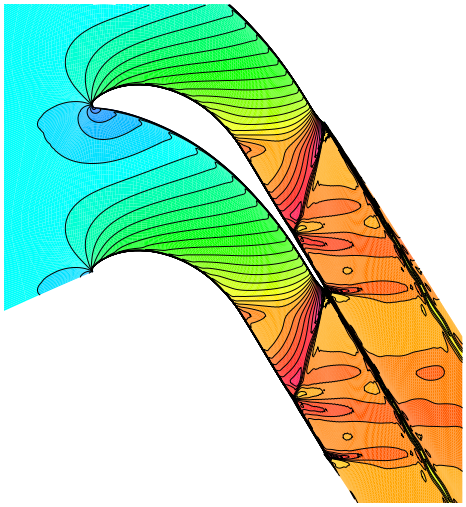

(b) laminar flow model, Mach number isolines, the presented cell-vertex method

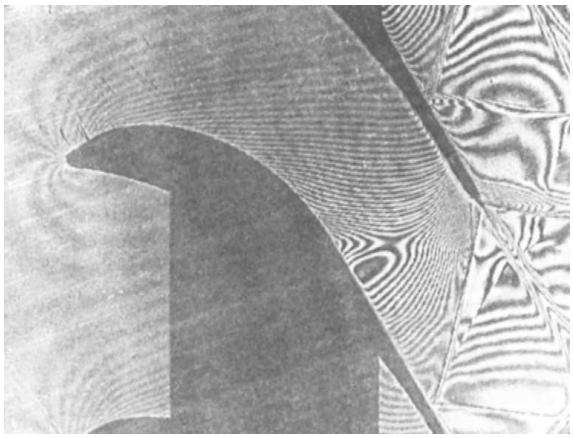

(c) interferogram, Šťastný and Šafařík [62]

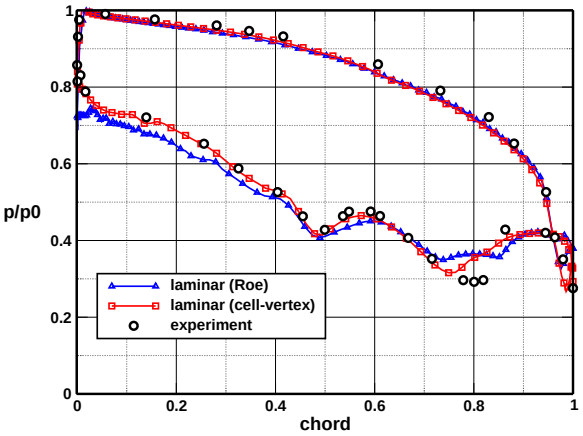

(d) distribution of pressure along profile

Figure 5: The flow in SE1050 turbine cascade

4.6 3D curved channel

The secondary flow with two counter-rotating vortices in a curved duct can be found in almost each fluid mechanics textbook. Later investigations, done e.g. by Bara et al [7], have discovered next pair of counter-rotating vortices for the flow with higher Dean numbers $De = Re/\sqrt{C}$, where $C = R/d_h$ is non-dimensional radius, R the inner radius and d_h the hydraulic diameter. The margin between two- and four-vortex structures is called critical Dean number (it is a function of C).

All calculations presented in this section were done for Dean numbers close to critical value, i.e. for small Reynolds numbers, where the use of laminar flow model is appropriate. The results of the former cell-vertex method are compared with the results of the Runge-

Kutta multistage scheme for steady incompressible laminar flow (Fořt et al [23]).

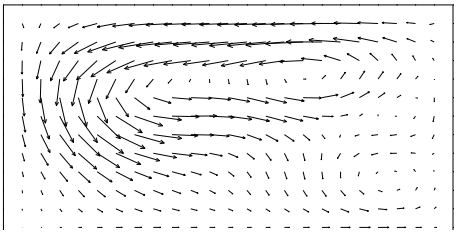

(a) cell-vertex scheme

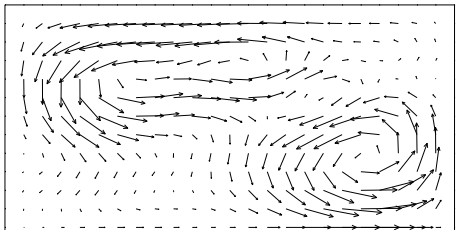

(b) cell-vertex scheme (lower artificial dissipation)

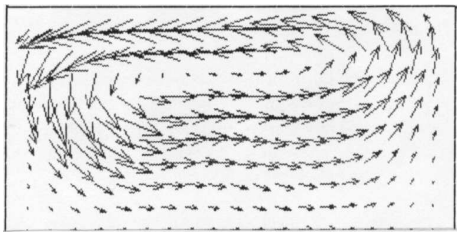

(c) Runge-Kutta scheme (Fořt et al [23])

Figure 6: The secondary flow structure, $De = 316 < De_c$, $C = 2.5$ and $\alpha = 140°$.

A curved channel with the constant square cross-section, turning angle 180° (0° corresponds to the inlet and 180° to the outlet) and inner radius equal to 1 has been used for all calculations. Numerical tests have shown that the flow field is very sensitive to the parameters of numerical methods such as the amount of artificial velocity, see Fig. 6. The big anti-clockwise rotating vortex in the Fig. 6.a has the same position like the one in Fig. 6.c. The clockwise rotating vortex is negligible. There is another anti-clockwise rotating vortex in the lower right corner, which rapidly increases its strength in the case of lower amount of artificial viscosity, see Fig. 6.b. The clockwise rotating vortex in Fig.6.b is stronger and shifted a bit leftwards.

5 Unsteady inviscid transonic flow in axial stages

The promising results of the numerical study of the unsteady stator/rotor interaction done by a quasi 3D Euler code during the participation of author at Diploma course 1997-98 at VKI and mainly the new experimental data, which were gathered at VKI's CT3 facility and which provide a good database for a validation of 3D unsteady numerical simulations, have led to a decision to develop the own 3D Euler code in order to better understand which unsteady effect is of potential and which is of viscous nature.

Numerical solution of the unsteady stator-rotor interaction brings mainly these difficulties:

- due to the different number of blades in the stator and in the rotor cascades the periodicity conditions need a special treatment,

- the relative movement of cascades has to be handled,
- the gap between stator and the rotor is very narrow (less than blade chord), so there are problems at least with the grid generation.

For the periodicity we use the idea of Rai and Madavan [54] and Dawes [10], i.e. we use a computational domain composed of m stator and n rotor pitches, where $mP_S = nP_R$ and m and n are small integers, see Fig. 7. The periodicity conditions are then given by equations (9)

$$\begin{aligned} \mathbf{W}(A) &= \mathbf{W}(B), \\ \mathbf{W}(C) &= \mathbf{W}(D), \end{aligned} \tag{9}$$

and do not require any special implementation.

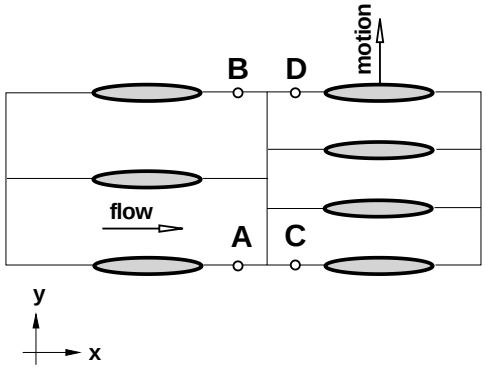

Figure 7: A computational domain composed of $m = 2$ stator and $n = 3$ rotor pitches.

The use of any kind of boundary condition along the stator-rotor interface is avoided by applying a relatively simple technique of 'interface cells', proposed by Giles [33] and [34]. Both stator and rotor grids have the same number of uniformly spaced points along interface, so they can be connected directly by grid lines, see Fig. 8.

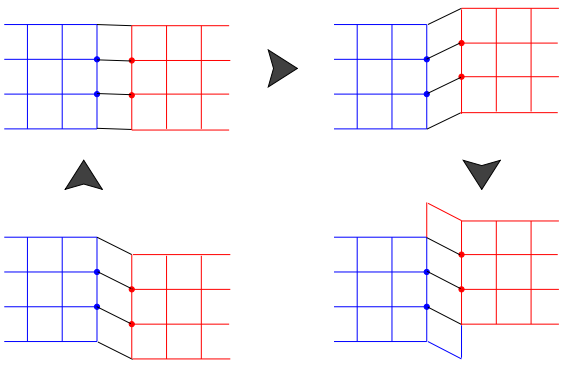

Figure 8: The interface between the stator and the rotor grid for an unsteady stage calculations.

Marked points denote the interface cell. The grids are overlapped over one cell row, therefore the same finite volumes (like for points inside the domain) can be used in points along the interface. The relative movement of grids is provided by the deformation of interface cells during the grid movement. The grids are periodically reconnected in a proper moment in order to avoid excessive cell deformation, see four consequent views in Fig. 8.

5.1 Unsteady flow in NASA stage

The NASA stage with 36 vanes and 64 blades published by Moffit et al [51] has been chosen for the first numerical tests. Calculations have been performed on the domain composed of three stator and five rotor blade passages, see Fig. 9, it corresponds to a stage with 36 vanes and 60 blades (number of vanes remained - the stator throat is kept).

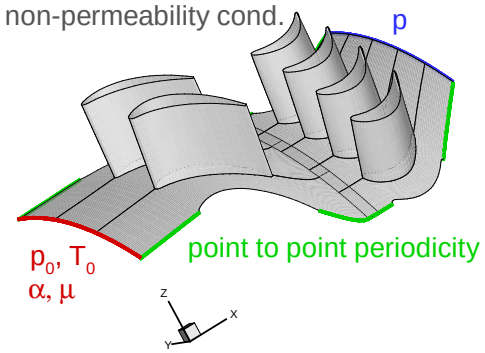

Figure 9: Computational domain and boundary conditions for an unsteady stage calculation (α and μ denote the pitch and yaw angle respectively).

The algebraic H-type grid for whole computational domain (3 stator and 5 rotor blade passages) amounts about 60 thousand points. The table 1 shows the comparison of measured (Moffit et al [51]) and calculated time-average flow angles and a mass flow rate. Symbols α and β denote the absolute and relative flow angles respectively. Index $\cdot_1$ is used for the stator exit and index $\cdot_2$ for the rotor exit. Calculated values of angles α_1 and β_2 fit very well the measured data. The higher calculated mass flow rate (no boundary layer blockage for an inviscid flow model) results in a slightly different angles α_2 and β_1.

	measured [51]	calculated
α_1 [°]	72.25	72.00
β_1 [°]	48.26	49.37
α_2 [°]	-22.60	-19.75
β_2 [°]	-56.40	-56.46
$\dot{m}$ $[kgs^{-1}]$	3.708	3.938

Table 1: The comparison of the time-pitch averages of flow angles at midspan and the comparison of mass flow rate

5.2 Unsteady flow in BRITE stage

The real stage is composed of 43 stator and 64 rotor blades. A domain composed of two stator and three rotor blade passages has been chosen as a good approximation, i.e. a slight change of the number of blades is necessary, either 42 stator and 63 rotor blades ('42/63' case) or 44 stator and 66 rotor blades ('44/66' case).

Two elliptical H-type computational grids with different number of points were generated by the 'JERRY' grid generation code of Arnone [1]. The 'basic' grid has about $4 \cdot 10^5$ points and the 'fine' grid about $6 \cdot 10^5$ points for the whole domain.

The time averaged distributions of M_{rel} fit very well the experiment (the agreement is better than for the numerical results published by Laumert et al [47], computed by the Navier-Stokes solver VOLSOL). The flow acceleration on a front part of the rotor suction side is well predicted at 15% and 50% (Fig. 10) and slightly over-predicted at 85% of the span.

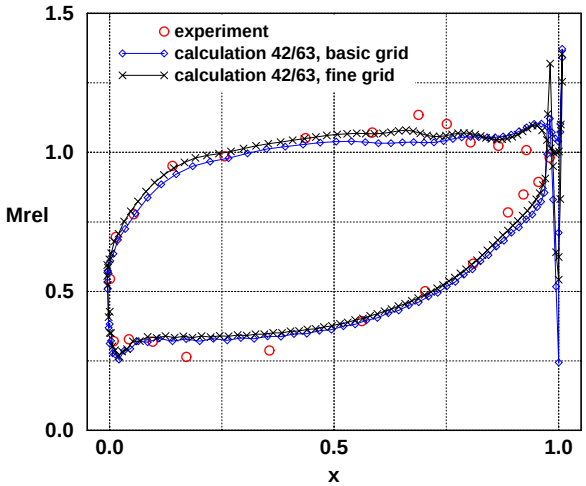

Figure 10: The time-averaged distribution of the relative Mach number around rotor blade at 50% of the span - comparison with the experimental data of VKI (Valenti et al [63]).

The example of unsteady results in form of static pressure traces for the 42/63 case on the basic grid is in the Fig. 11. The pressure traces for the particular probes in the

mentioned graph show the fluctuations with respect to the mean value (time average in considered probe location) and their plots are equidistantly distributed along y-axes. The computed unsteady results fit very well the experimental data (the agreement is again better than in Laumert et al [47]).

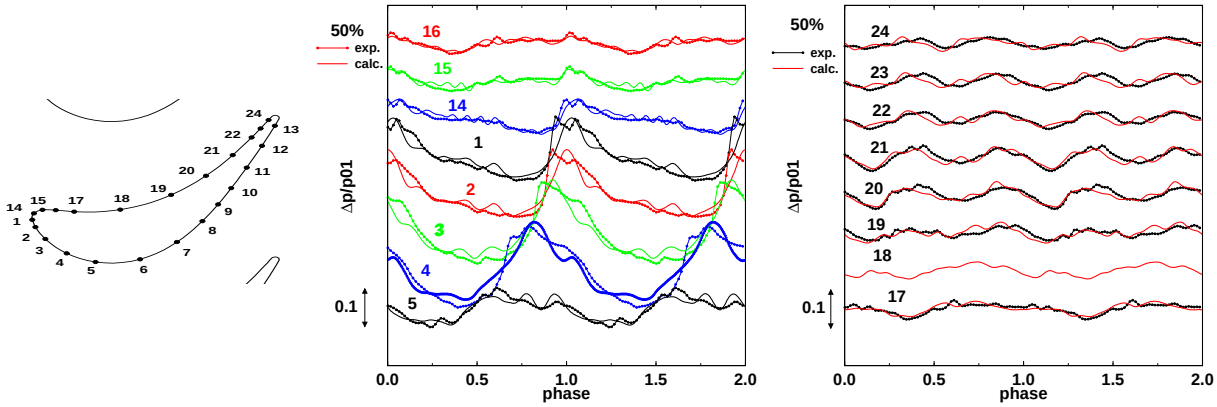

Figure 11: The time-resolved distribution of pressure at the specified locations on a rotor blade at 50% of the span - comparison with the experimental data of VKI (Valenti et al [63]).

6 Two-phase transonic flow of condensing steam

Condensation may appear during an expansion of vapor. The condensation itself is sometimes desired (e.g. for drying of earth gas through an expansion in nozzle) and sometimes undesired (e.g. it decreases the efficiency and durability of steam turbines). Condensation in turbomachinery applications is important issue mainly for the last stages of low–pressure part of steam turbine (used for production of electrical energy), since it is non-negligible loss source. Heat released by condensation in supersonic region may cause a steep pressure raise called condensation shock, which can be both steady or unsteady. Complex measurements on real turbine are complicated, therefore numerical predictions of condensation of transonic flow of wet steam yield valuable informations for the design of such turbines.

Presented flow model is an extension of Šejna's work [60]. The flow of the mixture is approximated by an inviscid or laminar flow models described by the quasi-2D and the 2D Euler or 2D Navier-Stokes equations respectively. We consider following simplifications for the modeling of liquid phase:

- condensation is homogenous,
- the droplets are convected by the vapor - there is a zero slip velocity between the mixture and the droplets,
- the steam has small wetness - volume of droplets can be neglected,
- the pressure of the mixture is approximated by the pressure of vapor,

- vapor is the perfect gas,
- droplets are described by the Hill's approximation [38].

The condensation process has two different mechanisms. The first one - a nucleation - is the creation of new droplets with radius equal to critical radius. We use the nucleation rate relation according to Becker and Döring [9]

$$J = \sqrt{\frac{2\sigma}{\pi m_v^3}} \cdot \frac{\rho_v^2}{\rho_l} \cdot \exp\left(-\beta \cdot \frac{4\pi r_c^2 \sigma}{3 k_B T_v}\right) \qquad [m^{-3}s^{-1}], \tag{10}$$

$$r_c = \frac{2\sigma}{\rho_l R_v T_v ln(p_v/p_s)} \qquad [m]. \tag{11}$$

The symbol σ denotes the surface tension of water (for straight surface), m_v the mass of one water molecule, ρ_v the vapor density, ρ_l the density of liquid phase, r_c the critical radius, k_B the Boltzmann constant, T_v the vapor temperature, R_v the gas constant, p_v the vapor pressure, and p_s the saturation pressure. The value of surface tension is corrected by the coefficient β, see Petr and Kolovratník [53]

$$\beta = 1.328 p_{cor}^{0.3} \pm 0.05, \tag{12}$$

where p_{cor} $[bar]$ denotes the pressure at the intersection of the expansion and steam saturation lines. We consider an isentropic expansion for this purpose, see Fig. 12.

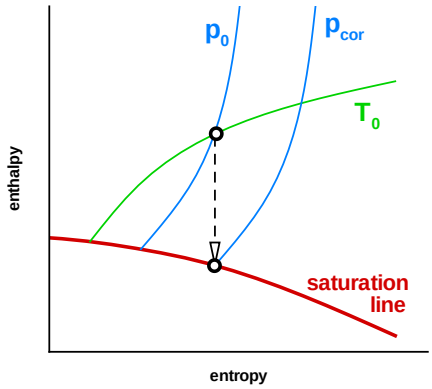

Figure 12: Calculation of p_{cor}.

The second mechanism is the growth $\dot{r}$ of already existing droplet (relation according to Valha [64])

$$\begin{aligned} \dot{r} &= \frac{\lambda_v \Delta T}{L\rho_l(1 + 3.18 \cdot Kn)} \cdot \frac{r - r_c}{r^2} \qquad [ms^{-1}], \\ Kn &= \frac{\eta_v \cdot \sqrt{2\pi R_v T_v}}{4 r p_v} \qquad [1], \end{aligned} \tag{13}$$

where λ_v is the vapor thermal conductivity, ΔT is the difference between temperature of vapor and liquid phase, r is the droplet radius, L is the latent heat of condensation, Kn is the Knudsen number and η_v is the vapor dynamic viscosity.

The Hill's approximation uses following three parameters for the whole droplet spectra:

$$Q_0 = n, \quad Q_1 = \sum_{i=1}^{n} r_i, \quad Q_2 = \sum_{i=1}^{n} r_i^2, \quad r = \begin{cases} 0, & w \leq 10^{-6} \\ \sqrt{Q_2/Q_0}, & w > 10^{-6} \end{cases}, \tag{14}$$

where n denotes the total number of droplets per unit mass of mixture, r_i is the radius of i-th droplet, r is the average radius and w is wetness - the mass fraction of liquid phase. The limit value 10^{-6} for wetness was chosen according to numerical tests in order to get stable numerical solution.

The Navier-Stokes equations for the 2D flow of mixture and the conservation law equations for Q_0, Q_1, Q_2 variables can be written together as one system of partial differential equations in conservative form (15)

$$\frac{\partial}{\partial t}\mathbf{W} = -\frac{\partial}{\partial x}\mathbf{F}^c + \frac{\partial}{\partial x}\mathbf{F}^v - \frac{\partial}{\partial y}\mathbf{G}^c + \frac{\partial}{\partial y}\mathbf{G}^v + \mathbf{Q}, \tag{15}$$

$$\begin{aligned}
\mathbf{W} &= [\rho, \rho u_x, \rho u_y, e, \rho w, \rho w Q_2, \rho w Q_1, \rho w Q_0]^T, \\
\mathbf{F}^c &= [\rho u_x, \rho u_x^2 + p, \rho u_x u_y, (e+p)u_x, \rho w u_x, \rho w Q_2 u_x, \rho w Q_1 u_x, \rho w Q_0 u_x]^T, \\
\mathbf{F}^v &= [0, \tau_{xx}, \tau_{xy}, u_x\tau_{xx} + u_y\tau_{xy} - q_x, 0, 0, 0, 0]^T, \\
\mathbf{G}^c &= \left[\rho u_y, \rho u_y u_x, \rho u_y^2 + p, (e+p)u_y, \rho w u_y \rho w Q_2 u_y, \rho w Q_1 u_y, \rho w Q_0 u_y\right]^T, \\
\mathbf{G}^v &= [0, \tau_{xy}, \tau_{yy}, u_x\tau_{xy} + u_y\tau_{yy} - q_y, 0, 0, 0, 0]^T, \\
\mathbf{Q} &= \left[0, 0, 0, 0, \rho\left(\tfrac{4}{3}\pi r_c^3 \rho_l \tfrac{J}{\rho} + \tfrac{4}{3}\pi 3 Q_2 \dot{r} \rho_l\right), \rho\left(r_c^2 \tfrac{J}{\rho} + 2Q_1\dot{r}\right), \rho\left(r_c \tfrac{J}{\rho} + Q_0\dot{r}\right), \rho\tfrac{J}{\rho}\right]^T,
\end{aligned} \tag{16}$$

where the symbol ρ denotes mixture density, u_x and u_y mixture velocity components, p pressure, e total energy of mixture per unit volume, τ shear stress, q heat flux, t time and x and y spatial coordinates. The first four and the last four equations are coupled by the equation for the pressure according to Šejna [60]:

$$p = (\gamma - 1)\frac{(1-w)}{1 + w(\gamma - 1)}\left[e - \frac{1}{2}\rho(u_x^2 + u_y^2) + \rho w L\right], \tag{17}$$

where $\gamma = \gamma(\mathbf{W})$ is the specific heat ratio. Numerical tests shown a better fit to experimental data if the specific heat ratio is considered as a local function of vector of unknowns $\gamma = \gamma(\mathbf{W})$ opposite to the case when it is considered as a constant (e.g.Šejna [60]).

The time step necessary for modeling of condensation corresponds to relaxation time τ, which is smaller than the time step suitable for convection. Basic concept of numerical method is described in Eq. (18). The convection part is solved by an explicit finite volume

cell-vertex method described in the third chapter. The condensation part is solved by the explicit two stage Runge-Kutta method. We have also tested one- and four-stage explicit Runge-Kutta methods, tests shown the two-stage method as a good choice.

$$\begin{aligned} &\frac{\partial}{\partial t}\mathbf{W} = \mathbf{Q} && \text{N steps } \frac{\Delta t}{2N} \text{ by RK-2 method,} \\ &\frac{\partial}{\partial t}\mathbf{W} = -\frac{\partial}{\partial x}\mathbf{F}^c + \frac{\partial}{\partial x}\mathbf{F}^v - \frac{\partial}{\partial y}\mathbf{G}^c + \frac{\partial}{\partial y}\mathbf{G}^v && \text{one step } \Delta t \text{ by cell-vertex m. ,} \\ &\frac{\partial}{\partial t}\mathbf{W} = \mathbf{Q} && \text{N steps } \frac{\Delta t}{2N} \text{ by RK-2 method,} \end{aligned} \tag{18}$$

where $N = \frac{\Delta t}{\tau}$.

As an initial conditions we usually prescribe the total inlet parameters (i.e. zero flow velocity) inside the whole domain. The boundary conditions are specified according to the different parts of boundary: we prescribe the total pressure and temperature, flow angle and $w = Q_i = 0$ at the subsonic inlet; the non-permeability or the no-slip together with adiabatic wall conditions for inviscid or laminar flow respectively; point-to-point periodicity; and the mean value of pressure or no condition at the turbine or the nozzle outlet respectively. Marching in time and using steady boundary conditions we get either a steady or a periodical unsteady solution. Presented method can be used also for unsteady cases.

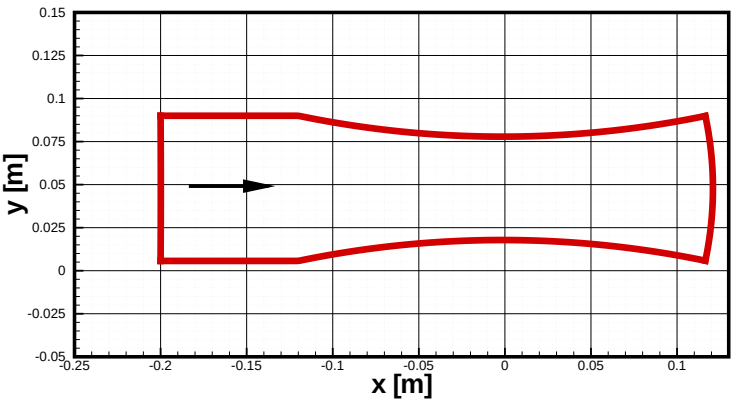

Figure 13: Barschdorff nozzle I [8] - computational domain

Figure 13 shows computational domain for the Barschdorff nozzle I [8]. Numerical results for two cases of inviscid two-phase flow in Barschdoff nozzle with the same inlet total pressure $p_{01} = 78390Pa$ and two different inlet total temperatures are shown in the Fig. 14. Heat released by the nucleation slows down the supersonic flow, resulting in pressure jump (called condensation shock). The position of nucleation start (i.e. the position of condensation shock) strongly depends also on used correction β (Eq. (12)). Such corrections are obtained from a set of experimental data. The pressure distributions in Fig.14 show a well captured position of nucleation start. The magnitude of pressure

rise for $T_{01} = 373.15K$ (Fig.14 on the right) is slightly over-predicted most probably due to used inviscid flow model (higher jump is expectable without physical viscosity).

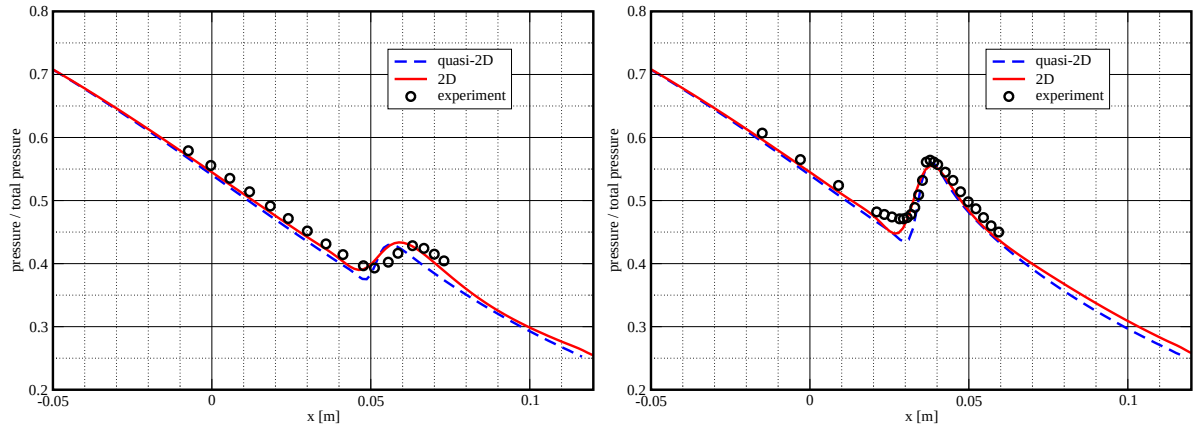

Figure 14: Pressure distribution along the Barschdorff nozzle axis, experimental data from Barschdorff [8], $T_{01} = 380.50K$ (on the left), $T_{01} = 373.15K$ (on the right).

The results of numerical tests for 2D transonic flow in a turbine cascade are also discussed.

7 Conclusions

The goals stated in the beginning of presented work were successfully fullfiled.

1. The finite difference methods for the linear scalar equations analyzed in the second chapter were used as a basis for all the presented finite volume methods. The favourable properties of the proposed finite difference method based on the splitting technique have been shown for the case of the convection-production equation. This finite difference method has been successfully used for the development of numerical method for the transonic flow of condensing steam.

2. The numerical method for the solution of 3D laminar transonic flow based on finite volumes of cell-vertex type for structured grid was developed and validated. During the method development were tested modifications of

   - inlet boundary condition: variants for 2D axial cascades, 2D radial cascades (combination of absolute and relative frame of reference in the case of rotor) and 3D axial cascades (the distribution of total relative parameters is considered for the rotor)
   - formulation of outlet boundary condition: constant value of pressure (it fails for the case with a bigger pressure gradients along the boundary, which are typical for transonic flow), non-reflecting condition of Giles for a steady flow

(rather complicated and limited to cell-vertex type of finite volumes and to axial cascades) and proposed 'integral of pressure' (comparable to non-reflecting condition, in addition suitable for any type of finite volumes and also for radial cascades)

- periodicity condition: common point to point periodicity and ghost cells for non-matched grids
- structured computational grid: algebraically generated H mesh (unphysical production of entropy at leading and trailing edge as a consequence of poor discretization of these regions), H mesh created from several parts obtained by elliptic generator, which are smoothed as a whole (unphysical production of entropy only at trailing edge), multi-block O-H mesh (unphysical production of entropy also at trailing suppressed thanks to nearly orthogonal mesh close to trailing edge and to grid coarsening downstream the trailing edge)

Numerical results of presented cell-vertex method were successfully verified using the numerical results of independent numerical methods of other authors as well as using the available experimental data. Obtained results were used in Škoda Energo enterprise and in PBS Velká Bíteš company. Results were also published on international conferences, e.g. Babák et al [6], Dobeš et al [13], Fořt et al [21], [22], [23], [24] and [25].

3. The numerical method for the solution of 3D unsteady inviscid stator/rotor interaction based also on finite volumes of cell-vertex type for structured grid was developed and validated.

   - the influence of deformation of interface cells as well as the influence of grid reconnection for the matching of stator and the rotor by 'interface cells' technique of Giles was tested (this influence was found negligible)

   Numerical results together with the experimental data of Von Kármán Institute were used for analysis of individual flow phenomena in stator/rotor interaction. Comparison of numerical results with the experimental data were published on international conferences, see Halama and Arts [35], Halama et al [36] and Valenti et al [63].

4. The numerical method for the solution of 2D two-phase transonic flow with condensation was developed and validated.

   - all material properties are taken as functions of temperature and/or pressure (e.g. specific heat ratio)
   - classical relation for nucleation is corrected according to Petr and Kolovratník
   - used fractional step method provides sufficiently robust numerical method and enables easy extension into 3D

- all terms describing condensation are treated strictly locally (small time steps are used only where it is necessary, i.e. extra computational time with respect to the case without condensation is reasonable)

Numerical results have been already published at international conference GAMM Jahres Tagung 2003 in Padua and are accepted for the International Workshop on Multiphase and Complex Flow Simulation for Industry in Cargèse 2003.

The development of presented numerical methods will further continue. The ideas for the future work are:

- to extend existing numerical methods for the turbulent flow by implementing an appropriate turbulence model;
- to develop an implicit or a semi-implicit numerical method;
- to extend the two-phase flow calculation into 3D case.

References

[1] Arnone A: Notes on the use of the JERRY and TOM grid generations codes, Firenze, November 1992.

[2] Arnone A., Pacciani R.: Rotor/stator interaction analysis using the Navier-Stokes equations and multigrid method, ASME Paper 95-GT-177.

[3] Arnone A., Pacciani R.: IGV-rotor interaction analysis in a transonic compressor using the Navier-Stokes equations, ASME Paper 96-GT-141.

[4] Arts T.: Etude de l'Ecoulement Tridimensionel dans Un Etage de Turbine Transsonique, Doctoral Thesis, VKI, July 1982.

[5] Arts T.: Three dimensional rotational inviscid flow calculation in axial turbine blade rows, Technical Note 154, VKI, September 1985.

[6] Babák M., Dobeš, J., Fořt, J., Fürst, J., Halama, J., Kozel, K., Kundera R.: Axial and radial cascades of small power turbines - comparisons of in-house and commercial flow solvers, Proceedings of seminar Topical problems of fluid mechanics 2002, ÚT AVČR, February 20, 2002, ISBN 80-85918-72-2, pp 5-8.

[7] Bara B., Nandakumar K., Masliah J.H.: An experimental and numerical study of the dean problem: flow development towards 2D multiple solutions, TASME - Journal of Fluid Mechanics, Vol.244, 1992, pp. 339-376.

[8] Barschdorff D.:, (1971), Verlauf der Zustandgrößen und gasdynamische Zuammenhänge der spontanen Kondensation reinen Wasserdampfes in Lavaldüsen, Forsch. Ing.-Wes., Vol. 37, No. 5, 1971, (in german).

[9] Becker R., Döring W.: Kinetische Behandlung der Keimbildung in übersättingten Dämpfen, Ann. d. Physik, 1935, B. 24, No. 8, (in german).

[10] Dawes W.N.: A numerical study of the interaction of a transonic compressor rotor overtip leakage vortex with the following stator blade row, ASME 94-GT-156.

[11] Dénos R.: Etude Aerodynamique et Thermique de l'Ecoulement Instationnaire Dans un Rotor de Turbine Transsonique, Doctoral Thesis, VKI, December 1996, (in english).

[12] Dobeš, J., Fořt, J., Fürst, J., Halama, J., Kozel, K.: Numerical solution of transonic flows in 2D and 3D axial and radial turbine cascades, 5th European conference on Turbomachinery, Prague, 2003.

[13] Dobeš, J., Fořt, J., Fürst, J., Halama, J., Kozel, K.: Numerical simulation of a flow for turbomachinery applications, Internal flows, vol. 1, ed. P. Doerfer, Proceedings of 5th International Symposium on Experimental and Computational Aerothermodynamics of Internal Flows, IFFM Publishers 2001, ISBN 83-88237-35-7, pp 297-304.

[14] Dobeš J., Fořt J.: Numerical solution of internal flow problems by upwind scheme on unstructured grid, Proceedigs of 4th Seminar Euler and Navier-Stokes equations, ÚT AVČR, May, 2001, ISBN 80-85918-65-X, pp 27-30.

[15] Dvořák R., Kozel K.: Mathematical models in aerodynamics, CTU Prague, 1996, (in czech).

[16] Dykas S., Goodheart K., Schnerr G.H.: Numerical study of accurate and efficient modelling for simulation of condensing flow in transonic steam turbines, 5th European conference on Turbomachinery, Prague 2003, pp 751-760.

[17] Erdos J.I., Alzner E., McNally W.: Numerical solution of periodic transonic flow through a fan stage, AIAA Journal, Vol.15, No.11, November 1977, pp 1559-1568.

[18] Fořt J.: private communication, 1997-2003.

[19] Fořt J., Kozel K., Vavřincová M.: Numerical simulation of steady and unsteady inviscid transonic flows by cell centered and cell certex schemes, Proceedings of the 5th Inetrnational Symposium on Computational Fluid Dynamics, Vol. I, pp 172 - 178, Japan Society of Comp. Fluid Dynamics, 1993.

[20] Fořt J., Fialová M., Fürst J., Horák M., Kozel K.: Numerical solution of several 2D and 3D internal flow problems, Proceedings of 15th Intenational Conference on Numerical Methods in Fluid Dynamics, Monterey, USA, Springer-Verlag, Berlin 1997, pp. 364-369

[21] Fořt J., Fürst J., Halama J., Hrušová M., Kozel K.: Comparison of cell centered and cell vertex finite volume methods for internal flow problems, International Series of Numerical Mathematics Vol. 129, Birkhäuser Verlag Basel/Switzerland, 1999, pp 325-332.

[22] Fořt J., Fürst J., Halama J., Kozel K.: Comparison of two finite volume methods for 3D transonic flows through axial cascades, Proceedings of 'Finite Volumes in Complex Applications II', Duisburg, 1999, pp 701-708.

[23] Fořt J., Fürst J., Halama J., Kozel K.: Numerical simulation of 3D subsonic and transonic internal flows, 16th IMACS world congress on scientific computation, applied mathematics and simulation, Lausanne Switzerland 2000, CD-ROM, ISBN 3-9522075-1-9.

[24] Fořt J., Fürst J., Halama J., Kozel K.: Computation of transonic flow through a radial and axial cascades, 20. Strömungstechnische Tagung des Instituts für Strömungsmechanik, TU Dresden 2000, ISBN 3-86005-256-X, pp 6-7.

[25] Fořt, J., Fürst, J., Halama, J., Kozel, K.: Numerical simulation of 3D transonic flow through cacades, Mathematica Bohemica, vol. 126, no. 2, 2001, pp 353-361.

[26] Fourmaux A.: Unsteady flow calculation in cascades, ASME Paper 86-GT-178.

[27] Fürst J.: private communication, 1997-2003.

[28] Fürst J., Kozel K.: Application of second order TVD and WENO schemes in internal aerodynamics, Journal of Scientific Computing, Vol. 17, No. 1-4, December 2001, ISSN 0885-7474.

[29] Giangiacomo P., Michelassi V., Martelli F.: Analysis of the mixing plane interface betweenstor and rotor of a transonic axial turbine stage, International Gas Turbines and Aeroengine Congress and Exhibition, Munich 2000, ASME Paper 2000-GT-634.

[30] Giles M.B.: Non-reflecting boundary conditions for the Euler equations, CFDL-TR-88-1, February 1988.

[31] Giles M.B.: Calculation of unsteady wake/rotor interaction, Journal of Propulsion Vol. 4, No. 4, 1988, pp 356-362.

[32] Giles M.B.: Non-reflecting boundary conditions for Euler equation calculations, AIAA Journal Vol. 28, No. 12, 1990, pp 2050-2058.

[33] Giles M.B.: Stator/rotor interaction in a transonic turbine, Journal of Propulsion Vol. 6, No. 5, 1990, pp 621-627.

[34] Giles M.B.: UNSFLO: A numerical method for the calculation of unsteady flow in turbomachinery, GLT Report No. 205, MIT, May 1991.

[35] Halama, J., Arts, T.: Numerical simulation of unsteady stator-rotor interaction, Proceedigs of 4th Seminar Euler and Navier-Stokes equations, ÚT AVČR, May, 2001, ISBN 80-85918-65-X, pp 41-44.

[36] Halama J., Arts T., Fořt, J.: Numerical solution of steady and unsteady transonic flow in turbine cascades and stages, AMIF 2002 conference, April 17-20, Lisbon. (to appear in journal 'Computers and fluids')

[37] Heiler M.: Instationäre Phänomene in homogen/heterogen kondensierenden Düsen- und Turbinenströmungen, Doctoral thesis, Uni Karlsruhe, 1999, (in german).

[38] Hill P.G.: Condensation of water vapor during supersonic expansion in nozzles, part 3, Journal of Fluid Mechanics, Vol.3, 1966, 593–620.

[39] Hoffman K.A., Chiang S.T.L., Siddiqui M.S., Papadakis M.: Fundamental equations of fluid mechanics, Engineering education system, Wichita, Kansas, May 1996, ISBN 0-9623731-9-2.

[40] Jameson A.: Solution of the Euler equations for two-dimensional transonic flows by a multigrid method, applied math. and computations, Vol. 13, 1983, pp 327-355.

[41] Jameson A.: Transonic flow calculations, MAE Report No. 1651, Princeton University, Princeton, New Jersey, 1984.

[42] Jung A.R., Mayer J.F., Stetter H.: Simulation of 3D unsteady stator/rotor interaction in turbomachinery stages of arbitrary pitch ratio, ASME Paper 96-GT-69.

[43] Kapteijn C., Amecke J., Michelassi V.: Aerodynamic performance of a transonic turbine guide vane with trailing edge coolant ejection: Part I - experimental spproach, Journal of Turbomachinery Vol.118, July 1996, pp 519-528.

[44] Kolovratník M.: A contribution to problem of creation of liquid phase during steam expansion, Doctoral thesis, Prague 1993, (in czech).

[45] Kozel K., Fořt J.: Modern finite volume methods solving internal flow problems, Seminar / Summer School CFD for Turbomachinery Applications, Gdansk, September 1-3, 2001, pp 124-139.

[46] Kozel K., Fořt J.: Modern finite volume methods solving internal flow problems, Task Quarterly, pp 127-142, Task Publishing Gdansk, Poland, January 2002, ISBN 83-87359-57-2.

[47] Laumert B., Mårtensson H., Fransson T.H.: Investigation of the flow field in the transonic VKI BRITE EURAM turbine stage with 3D steady and unsteady N-S computations, ASME Paper 2000-GT-433, ASME TURBOEXPO 2000, Munich.

[48] Léonard O.: Conception et Développement d'Une Méthode Inverse de Type Euler et Application à la Génération de Grilles d'Aubes Transsoniques, Doctoral Thesis, VKI, March 1992, (in french).

[49] LeVeque R. J.: Numerical methods for conservation laws, Birkhäuser 1999, ISBN 3-7643-2723-5.

[50] Magagnato F., Rachwalski J., Gabi M.: An application of the buffer layer technique to computations of flow in turbomachinery, Proceedings of Conference on Modelling fluid flow 2003, Budapest.

[51] Moffit T.P., Szanca E.M., Whitney W.J., Behning F.P.: Design and cold-air test of single uncooled core turbine with high work output, NASA Technical paper 1680, Lewis Research Center, Cleveland, Ohio, 1980.

[52] Paniagua G., Dénos R., Arts T.: Steady-unsteady measurement of the flowfield downstream of a transonic HP turbine stage, offered at 4-th European Conference on Turbomachinery Fluid Dynamics and Thermodynamics, Florence, Italy, 2001.

[53] Petr V., Kolovratník M.:Heterogeneous Effects in the Droplet Nucleation Process in LP Steam Turbines", 4th European Conference on Turbomachinery, Firenze 2001, Italy.

[54] Rai M.M., Madavan N.K.: Multi-airfoil Navier-Stokes simulations of turbine rotor-stator intercation, Journal of turbomachinery, Vol 112, pp 377-384.

[55] Saxer A.P.:A numerical analysis of 3D inviscid stator/rotor interaction using non-reflecting boundary conditions, Report GTL No. 209, March 1992.

[56] Schnerr G.H., Winkler G.: Shock/boundary layer interaction in dispersed transonic two-phase flow, Proceedings of 5th ISAIF, Gdansk 2001, pp 429-442, ISBN 83-88237-35-7.

[57] Sopuch P.: Kinetics of phase change vapor–liquid and its numerical simulation, Doctoral thesis, IT CAS CR, Prague, 1996, (in czech).

[58] Strang G.: On the construction and comparison of difference schemes, SIAM Journal of Numerical Analysis, Vol. 5, 1968, pp 506-517.

[59] Stringer S.M., Morton K.W.: Artificial viscosity for the cell vertex method, Report no. 96/08, Oxford University Computing Laboratory, April 1996.

[60] Šejna M.: Numerical medelling of two–phase flow of steam with homogenous condensation, Doctoral thesis, Prague 1995, (in czech).

[61] Shapiro A.H.: The dynamics and thermodynamics of compressible fluid flow, Vol. I, New York, The Ronald Press Co, 1953.

[62] Šťastný M., Šafařík P.: Boundary layer effects on the transonic flow in a straight turbine cascade, ASME Paper 92-GT-155.

[63] Valenti E., Halama J., Dénos R., Arts T.: Investigation of the 3D unsteady rotor pressure field in a HP turbine stage, ASME Paper GT-2002-30365, Proceedings of ASME TURBO EXPO 2002, June 3-6 2002, Amsterdam.

[64] Valha J.: The flow of wet steam in through–flow part of steam turbine, Doctoral thesis, SVUSS Běchovice, 1988, (in czech).

[65] Vavra M.H.: Aerothermodynamics and flow in turbomachines, R.E. Krieger Publishing Company, 1974.

[66] Young J.B.: Two-Dimensional, Nonequilibrium, Wet–Steam Calculations for Nozzles and Turbine Cascades, Journal of Turbomachinery, Vol. 114, July 1992.